Spectrochimica Acta Part A: Molecular and Biomolecular Spectroscopy 360 (2026) 128016



Contents lists available at ScienceDirect

Spectrochimica Acta Part A:
Molecular and Biomolecular Spectroscopy

journal homepage: www.journals.elsevier.com/spectrochimica-acta-part-a-molecular-and-biomolecular-spectroscopy





Direct microRNA detection via topologically engineered CRISPR/Cas12a cascade amplification assay

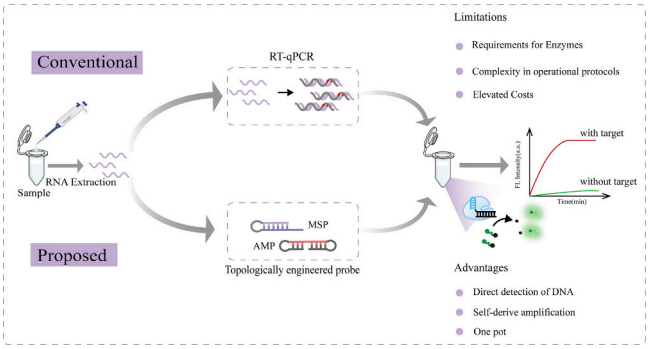
Meng Shen [a,1], Peiying Zhang [a,1], Lihua Ding [a], Xiaonan Yang [b], Leiliang He [a], Yongjun Wu [a], Songcheng Yu [a,*]

[a] College of Public Health, Zhengzhou University, Zhengzhou 450001, China
[b] School of Electrical and Information Engineering, Zhengzhou University, Zhengzhou 450001, China

HIGHLIGHTS

- DNA topological engineering enables programmable control of CRISPR/Cas12a activation.
- A self-driven cascade amplification circuit is established using CRISPR/Cas12a trans-cleavage.
- Direct RNA detection is achieved by CRISPR/Cas12a without reverse transcription.

GRAPHICAL ABSTRACT



ARTICLE INFO

Keywords:
CRISPR/Cas12a
RNA
Target-amplification-free
Cascade

ABSTRACT

The CRISPR/Cas12a system has emerged as a powerful tool for biosensing due to its high specificity, sensitivity and programmability. However, direct RNA detection is hindered by its inherent DNA-targeting trans-cleavage activity, which typically necessitates a reverse transcription amplification to convert RNA into DNA. Herein, we report a one-pot assay that enables direct detection of microRNA-21 without target amplification. The method employs a molecular switch probe (MSP) that recognizes miRNA-21 and activates Cas12a activity, along with an amplifier probe (AMP) that establishes a self-driven cascade signal amplification. This biosensor achieves a detection limit of 2.88 pM, with high accuracy (recovery of 95.5%–108.6%) and good precision (RSD: 2.35%–7.18%), and exhibits excellent specificity against homologous miRNAs. Using this assay, we successfully quantified the elevated levels of miRNA-21 in lung squamous carcinoma (H520) cells compared to normal bronchial epithelial cells (BEAS-2B). Furthermore, a methodological comparison with RT-qPCR revealed a similar trend between the two methods. This study provides a simple and reliable strategy for direct RNA detection using CRISPR/Cas12a.

* Corresponding author at: 100 Kexue Avenue, Zhengzhou City, China.
E-mail address: scyu@zzu.edu.cn (S. Yu).
[1] These authors contributed equally to this work.

https://doi.org/10.1016/j.saa.2026.128016
Received 4 January 2026; Received in revised form 26 April 2026; Accepted 28 April 2026
Available online 29 April 2026
1386-1425/© 2026 Elsevier B.V. All rights are reserved, including those for text and data mining, AI training, and similar technologies.

1. Introduction

MicroRNAs (miRNAs) are small, non-coding RNA molecules of approximately 21–24 nucleotides in length. They play pivotal roles in the post-transcriptional regulation of gene expression [1,2]. MiRNAs recognize target mRNAs primarily through imperfect base pairing with the 3'-UTRs, thereby mediating translational repression or mRNA degradation. This fine-tuning mechanism regulates approximately 30% of human genes [3–5]. The sophisticated regulatory networks governed by miRNAs are integral to fundamental cellular processes, including proliferation, differentiation, apoptosis, and development [6]. Consequently, dysregulation of miRNA expression is intimately linked to the pathogenesis of various human diseases [7], particularly cancer [8].

Among the numerous cancer-associated miRNAs, microRNA-21 (miRNA-21) has emerged as the most consistently overexpressed one across diverse cancers including lung, breast, colorectal, pancreatic, and bladder carcinomas [9,10]. Functionally, miRNA-21 exerts its oncogenic effects by targeting critical tumor suppressors such as PTEN, PDCD4, and TPM1, thereby enhancing cell survival, proliferation, and invasion while suppressing apoptosis [11,12]. The consistent upregulation of miRNA-21 in malignant tissues, combined with its remarkable stability in various body fluids including serum, plasma and urine, has positioned miRNA-21 as an exceptionally attractive minimally invasive biomarker for cancer diagnosis, prognosis and therapeutic monitoring.

Detection of miRNA-21 faces formidable challenges arising from its intrinsic properties: short length, low abundance, high sequence homology, and subtle expression differentials between pathological and physiological states [13]. These characteristics impose profound technical constraints on conventional analytical methods. Northern blotting suffers from inadequate sensitivity, substantial sample consumption, and protracted processing times [14]. Microarray technology, despite enabling high-throughput profiling, proves ineffective in distinguishing highly conserved miRNA family members [15]. Although reverse transcription quantitative PCR (RT-qPCR) offers exceptional sensitivity and quantitative capability, it suffers from variable reverse transcription efficiency, demanding primer design requirements and instrumentation dependency. These limitations preclude its utility in resource-constrained environments or point-of-care testing (POCT) scenarios [16]. Isothermal amplification strategies, including rolling circle amplification (RCA), loop-mediated isothermal amplification (LAMP), and strand displacement amplification (SDA), have emerged as viable PCR alternatives that circumvent thermal cycling while enhancing analytical sensitivity [17]. However, these isothermal amplification techniques still rely on reverse transcription for converting miRNA targets into DNA templates [18]. These requirements adds extra operational complexity, potential systematic bias and increased vulnerability to non-specific amplification and false positives in low-abundance samples.

Clustered Regularly Interspaced Short Palindromic Repeats (CRISPR) constitute an adaptive immune system inherent to prokaryotes [19]. CRISPR-associated (Cas) proteins are broadly categorized into two classes (Class 1 and Class 2) [20]. Owing to their simplified protein composition, Class 2 Cas proteins have garnered notably more research interest and found wider application than their Class 1 counterparts [21]. Within the Class 2 family, Cas12a exhibits a lower molecular weight and utilizes a shorter crRNA compared with other Cas proteins [22]. Furthermore, unlike Cas13a which trans-cleaves single-stranded RNA (ssRNA) substrates [23], Cas12a exhibits trans-cleavage activity against single-stranded DNA (ssDNA), thereby offering enhanced substrate stability and substantial cost advantages.

However, it is precisely the DNA-targeting nature of Cas12a that necessitates an additional conversion step when detecting miRNA (e.g., reverse transcription). To address this issue, researchers have developed innovative split crRNA designs that enable direct RNA detection without reverse transcription [24,25]. These engineered systems achieve highly sensitive RNA detection by replacing the crRNA spacer with a complementary split segment, which reconstitutes Cas12a activity upon target RNA binding. Similarly, the split sgRNA strategy has been extended to Cas12b and successfully applied to direct microRNA detection in clinical samples [26]. While these methods represent notable conceptual breakthroughs, many of them require multi-step workflows, external DNA activators, or remain challenging to implement in a simple one-pot format without compromising sensitivity.

To overcome the fundamental limitations mentioned above, we developed a one-pot assay that enables direct detection of miRNA-21 through topological engineering of specialized DNA probes. Our design strategy centers on the conceptual innovation of bypassing reverse transcription amplification through the creation of a molecular circuit that directly converts the presence of target miRNA into Cas12a activation and achieves cascade signal amplification. This approach represents a paradigm shift from conventional CRISPR-based RNA detection methods by establishing a direct interface between native miRNA molecules and the DNA-targeting CRISPR/Cas12a system through sophisticated nucleic acid nanotechnology. This one-pot CRISPR/Cas12a assay employing self-driven cascade signal amplification enables direct, simple, rapid, and accurate miRNA detection, providing a preliminary foundation for clinical diagnostic exploration.

2. Materials and methods

2.1. Oligonucleotides and materials

All the DNA and RNA oligonucleotides were obtained from Sangon Biotechnology Co., Ltd. (Shanghai, China). All the sequences of DNA and RNA oligonucleotides are listed in Table S1. LbCas12a nuclease and ssDNA reporter labeled with 6-FAM and BHQ-1 were purchased from Editgene Co., Ltd. (Guangzhou, China). The 10× cleavage buffer r2.1 (50 mM NaCl, 10 mM Tris-HCl, 10 mM MgCl2, pH 7.9) was used for CRISPR/Cas12a reactions.

2.2. Feasibility validation of probe activation

2.2.1. Sensing of miRNA-21 by MSP

To verify whether miRNA-21 could open MSP to achieve strand displacement, a total of 10 μL mixture was prepared by mixing 1 μL of 5 μM miRNA-21, 2 μL of 5 μM MSP and 7 μL hybridization buffer (containing 20 mM Tris-HCl, 0.1 M NaCl, and 10 mM $MgCl_2{\cdot}6H_2O$). After incubation at room temperature, the mixture was analyzed by a 15% polyacrylamide gel using 1 × TBE as the electrophoresis buffer with a constant voltage of 110 V for 90 min. The gel was imaged using a Gel Doc XR+ system from Bio-Rad company (California, USA).

2.2.2. Activation of CRISPR/Cas12a by MSP

To verify whether MSP can activate Cas12a upon opening, we mixed 1 μL of 5 μM miRNA-21 with 2 μL of 5 μM MSP for incubation at room temperature. Subsequently, this mixture was added to a solution containing 1 μL of 1 μM Cas12a, 0.5 μL of 1 μM crRNA1, 2 μL of 10 × Cas12a cleavage buffer, 1 μL of 10 μM reporter, and 12.5 μL of nuclease-free water to bring the total reaction volume to 20 μL. After incubation at 30 °C for 1 h, the fluorescence signal was measured at $\lambda_{ex}/\lambda_{em}$ = 480/520 nm.

2.2.3. Signal amplification effect of AMP

To investigate the amplification effect of the AMP on the fluorescence intensity of the CRISPR/Cas12a system, a comparison was made between the fluorescence intensities of the CRISPR system with an AMP probe and those without the AMP probe. Initially, we combined 2 μL of 10 nM Activator A, 1 μL of 1 μM Cas12a, 0.5 μL of 1 μM crRNA1, 2 μL of 10× Cas12a cleavage buffer, 1 μL of 10 μM reporter, and 3 μL of 100 nM AMP probe in a tube and mixed thoroughly by pipetting. Subsequently, 0.5 μL of 1 μM crRNA2 was added, and the reaction mixture was brought to a final volume of 20 μL with 10 μL of DEPC-treated water. The

QuantStudio 1 Plus real-time PCR system from Thermo Fisher Scientific (Massachusetts, USA) was utilized for monitoring fluorescence signal at $\lambda_{ex}/\lambda_{em}$ = 480/520 nm every 30 s at 30 °C.

2.2.4. Detection of miRNA-21 with AMP

After verifying the success of the strand displacement and AMP signal amplification individually, they were integrated to validate the overall feasibility. 2 μL of miRNA-21 sample was mixed with 1 μL of 100 nM MSP. Subsequently, 2 μL of 10× Cas12a cleavage buffer, 1 μL of 10 μM reporter, 3 μL of 100 nM AMP, 0.5 μL of 1 μM crRNA1, 0.5 μL of 1 μM crRNA2, 1 μL of 1 μM Cas12a protein, and 9 μL of nuclease-free water were added to make up a 20 μL reaction solution. Then, the QuantStudio 1 Plus real-time PCR system from Thermo Fisher Scientific was utilized for monitoring fluorescence signal at $\lambda_{ex}/\lambda_{em}$ = 480/520 nm every 30 s at 30 °C.

2.3. Condition optimization

After verifying the signal amplification function of the established method, we further improved the signal-to-noise(S/N) ratio by systematically optimizing reaction components, including the concentrations of AMP(1–20 nM), MSP(2.5–50 nM), reporter(500–2500 nM), and Cas12a(5–60 nM), as well as the incubation time(5–60 min). The optimal conditions were selected for the procedures of miRNA-21 detection.

2.4. The procedures of miRNA-21 detection

2 μL of sample containing miRNA-21 was mixed with 1 μL of 100 nM MSP. Subsequently, 2 μL of 10× Cas12a cleavage buffer, 2 μL of 15 μM reporter, 3 μL of 100 nM AMP, 0.5 μL of 1 μM crRNA1, 0.5 μL of 1 μM crRNA2, 1 μL of 1 μM Cas12a protein, and 8 μL of nuclease-free water were added to make up a 20 μL reaction solution, which was incubated at 30 °C for 30 min. Then, the fluorescence intensity was recorded at $\lambda_{ex}/\lambda_{em}$ = 480/520 nm.

2.5. Detection of real sample

To assess the practical utility of the proposed sensor, quantification of miRNA-21 expression was performed in two distinct bronchial epithelial cell lines, the normal BEAS-2B cells and the human lung squamous carcinoma H520 cells. BEAS-2B cells were maintained in DMEM medium supplemented with 10% (*v*/v) fetal bovine serum (FBS), while H520 cells were cultured in RPMI 1640 medium containing 10% (v/v) FBS. All cell lines were incubated at 37 °C under a humidified atmosphere of 5% CO_2. Following standardized cell harvesting procedures, total RNA was isolated from cell lysates using the Trizol reagent kit from Accurate Biotechnology (Changsha, China) according to the manufacturer's protocol. The extracted RNA samples were subsequently detected by the proposed sensor according to the described procedures of miRNA-21 detection.

3. Results and discussion

3.1. Detection mechanism

In this study, we propose a method for direct detection of miRNA-21 utilizing the CRISPR/Cas12a system, which is engineered with two functionally integrated DNA probes. The core innovation lies in the strategic application of a toehold-mediated MSP and a dumbbell-shaped amplifier probe (AMP) to eliminate the need for reverse transcription amplification and to enable a one-pot and isothermal assay with self-driven cascade signal amplification (Fig. 1). It should be noted that the signal amplification via the AMP probe is used solely for sensitivity enhancement and does not constitute target pre-amplification (e.g., PCR or LAMP).

The MSP is a single-stranded DNA molecule engineered into a stem-loop (hairpin) structure, which comprises two critical functional domains. The stem region is designed with a toehold sequence complementary to the target miRNA-21, serving as the initial recognition and binding site. The loop domain contains a specific sequence capable of activating the CRISPR/Cas12a system mediated by crRNA1. Simultaneously, the dumbbell-shaped AMP, a second single-stranded DNA probe, is designed with a central functional domain flanked by two looped connection regions. The central domain possesses a Cas12a activator sequence mediated by crRNA2. However, in its native state, this activator is effectively silenced because it is hybridized intramolecularly with complementary sequences from the 5′ and 3′ ends of the same probe to form a double-stranded structure that is inaccessible for Cas12a activation. The looped connection regions are single-stranded DNA that serve as substrates for the trans-cleavage activity of Cas12a.

In the absence of the target miRNA-21, the MSP maintains its stable hairpin conformation. This closed structure sterically hinders the activator sequence in the loop to prevent it from binding to and activating

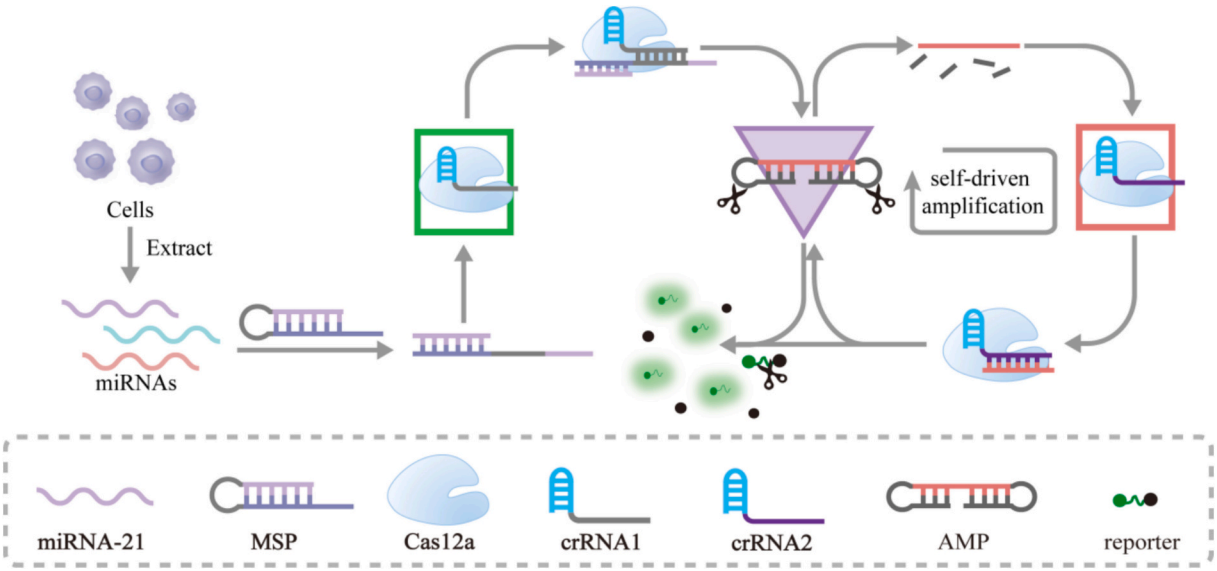


Fig. 1. Mechanism illustration of direct detection of miRNA-21 via topological engineering.

the Cas12a-crRNA1 complex, which results in minimal background signal. The presence of target miRNA-21 initiates a toehold-mediated strand displacement reaction. The miRNA-21 binds to the toehold region of the MSP and subsequently unfolds the stem to force the hairpin into an open conformation. This structural transition exposes the previously sequestered activator sequence within the loop to allow it to bind to the Cas12a-crRNA1 complex. This binding event triggers the trans-cleavage activity of the activated Cas12a enzyme.

Subsequently, the mechanism enters a signal amplification cascade once Cas12a is activated by the miRNA-21-opened MSP. The activated Cas12a-crRNA1 complex performs two concurrent actions. On one hand, it trans-cleaves fluorescent reporter probes labeled with fluorophore-quencher to generate an initial fluorescent signal. On the other hand, and critically for amplification, it trans-cleaves the ssDNA loops of the AMP. This cleavage event disrupts the structural integrity of the dumbbell probe to dissociate its self-hybridized ends. This dissociation liberates the central activator sequence to bind to the Cas12a-crRNA2 complex, which in turn trans-cleaves more fluorescent reporter probes and AMP probes to generate more fluorescent signal and to release even more activator sequences. This establishes a positive feedback loop, named self-driven cascade signal amplification circuit, which dramatically amplifies the fluorescent signal output. The intensity of the final fluorescence signal is directly proportional to the initial concentration of target miRNA-21 to enable its quantitative detection.

In this method, we leverage rational topological engineering of DNA probes, MSP for target sensing and AMP for signal amplification, which are seamlessly integrated with the properties of the CRISPR/Cas12a system. This design achieves direct, sensitive and specific detection of miRNA-21 without the prerequisite of RNA-to-DNA reverse transcription and extra amplification.

3.2. Feasibility validation of probe activation

The MSP features an 8-nucleotide (nt) toehold sequence within its stem region, adjacent to a domain fully complementary to miRNA-21. The loop contains the crRNA1 recognition sequence. Hybridization of miRNA-21 to its complementary domain initiates toehold-mediated strand displacement, unfolding the MSP and exposing the loop region. Gel electrophoresis analysis confirmed the MSP-miRNA-21 binding interaction. As depicted in Fig. 2A (lane 3), hybridization yielded a new band exhibiting markedly reduced electrophoretic mobility compared with the unbound MSP control, consistent with the formation of a higher molecular weight complex. This observation was corroborated by comparative fluorescence intensity measurements, which verified the exposure of Activator A upon miRNA-21 binding (Fig. 2B).

Subsequently, the Cas12a/crRNA1 complex recognized the exposed loop sequence of the MSP to trigger its trans-cleavage activity. This enzymatic activity cleaved both the fluorescently labeled single-stranded DNA (ssDNA) reporter and the loop sequences (5'-CCCCC-3′) located at each terminus of the adjacent AMP. Prior to cleavage, the AMP adopted a double-stranded DNA (dsDNA) structure with dual stem-loop motifs upon annealing, residing in a thermodynamically metastable state. Cleavage of the AMP loops drastically reduced the melting temperature (Tm) of the AMP structure. Consequently, the destabilized AMP

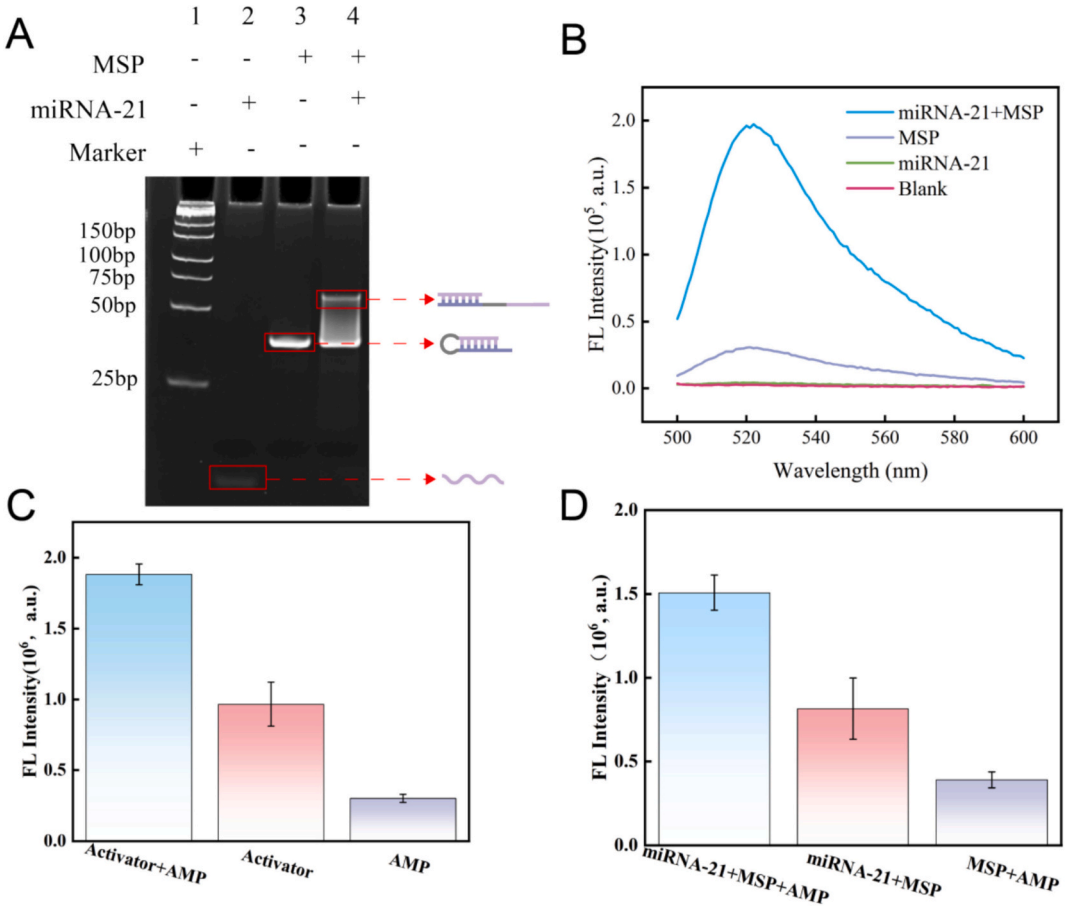


Fig. 2. Feasibility analysis of CRISPR/Cas12a-mediated self-driven cascade for detection of miRNA-21 without target amplification. (A) Polyacrylamide gel electrophoresis analysis of binding between MSP and miRNA-21. The "+" represents the presence and the "-" represents the absence of the corresponding reagent. (B) Fluorescence intensity comparison to verify the Cas12a/crRNA1 activation by exposed MSP. (C) Verification of signal amplification by AMP. (D) The overall feasibility of detecting miRNA-21 when AMP is present (blue) and absent (purple). (Error bars represent standard deviation, SD; $n = 3$). (For interpretation of the references to colour in this figure legend, the reader is referred to the web version of this article.)

denatured to expose Activator B at the reaction temperature (30 °C) (Fig. S1 and S2). The exposed Activator B then activated the trans-cleavage activity of the Cas12a/crRNA2 complex (Fig. 2C). Ultimately, the collaborative trans-cleavage activities of Cas12a/crRNA1 and Cas12a/crRNA2 resulted in the amplified cleavage of reporter probes to generate a substantial fluorescent signal output (Fig. 2D). The kinetic curve is presented in Fig. S3.

3.3. Condition optimization

3.3.1. AMP concentration

As AMP concentration directly influences signal amplification, its optimization was prioritized. Fluorescence intensity exhibited a concentration-dependent increase within the tested range (Fig. 3A and B). The magnification factor reached its maximum at an AMP concentration of 15 nM, which was consequently selected for all subsequent experiments.

3.3.2. MSP concentration

MSP concentration governs the efficiency of Cas12a activation via miRNA-21 binding. Fluorescence signal intensity increased with rising MSP concentration (Fig. 3C). The optimal S/N ratio was observed at 5 nM MSP.

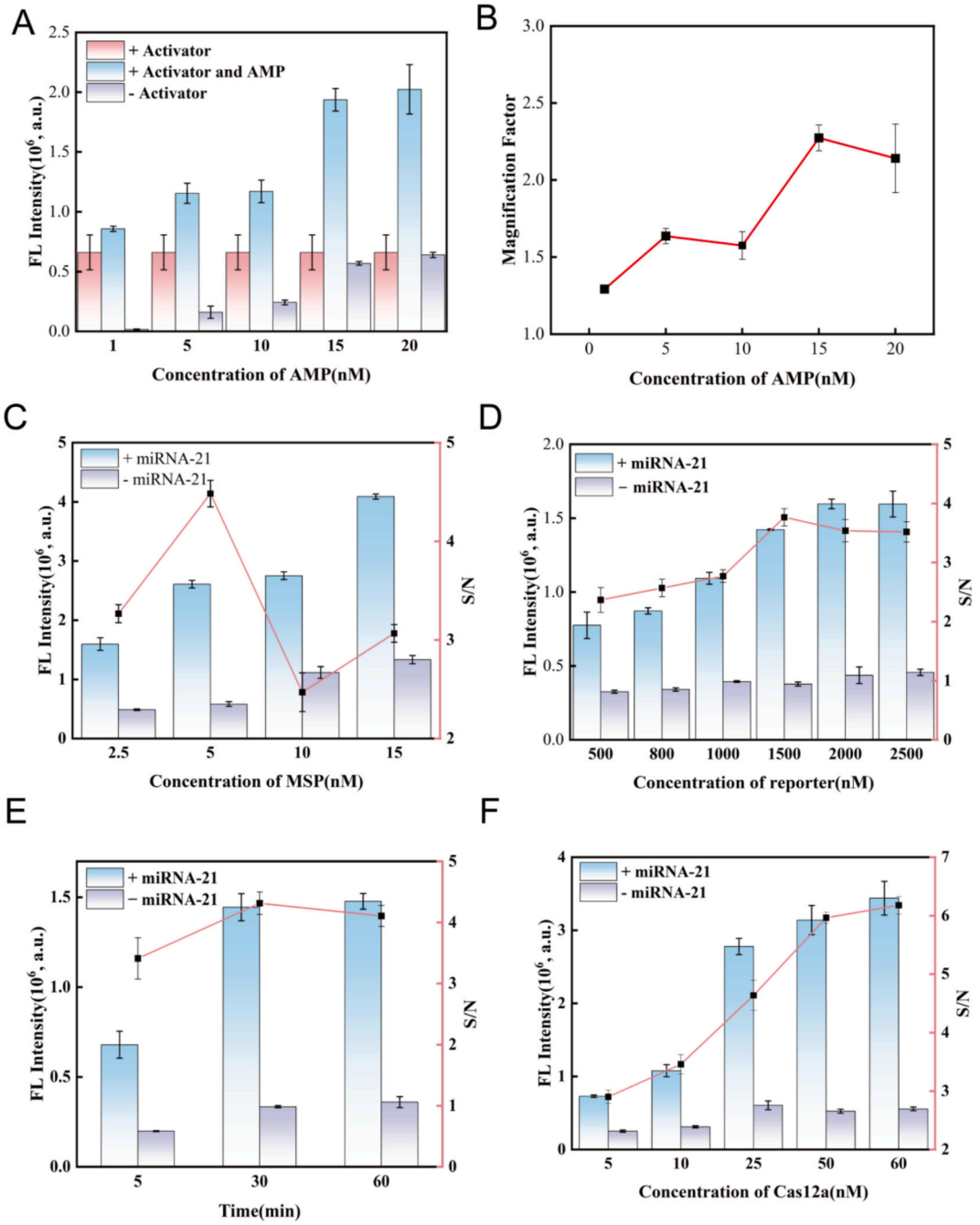


Fig. 3. Optimization of reaction conditions. (A) Effect of amplifier probe (AMP) concentration. (B) The magnification factor at different concentrations of AMP, where the magnification factor refers to the ratio of the experimental group minus the background signal to the positive control. (C) Effect of molecular switch probe (MSP) concentration. (D) Effect of reporter concentration. (E) Effect of Cas12a/crRNA1 trans-cleavage incubation time. (F) The impact of Cas12a protein concentration. (Error bars represent standard deviation, SD; $n = 3$).

3.3.3. Reporter concentration

The concentration of the fluorescently labeled ssDNA reporter probe is critical as the direct source of the detected signal. Fluorescent signals demonstrated a positive correlation with reporter probe concentration (Fig. 3D). The highest S/N ratio was achieved at a reporter concentration of 1500 nM.

3.3.4. Reaction time of Cas12a

The reaction time for Cas12a/crRNA-mediated trans-cleavage has been optimized. Fluorescence kinetics revealed a time-dependent increase in signal intensity (Fig. 3E). Peak S/N performance occurred at 30 min, which was adopted for subsequent assays.

3.3.5. Cas12a Concentration

Cas12a, a protein that forms a ternary complex with crRNA and the target, has a concentration that influences the generation of the overall fluorescence signal. Upon optimization, it was observed that the fluorescence signal increased with the elevation of Cas12a protein concentration, stabilizing after reaching 50 nM (Fig. 3F). Consequently, a concentration of 50 nM was selected for subsequent experiments.

3.4. Analytical performance

The analytical performance of the developed method for miRNA-21 detection was assessed under the optimized conditions (Fig. 4A). Fluorescence signal intensity exhibited a concentration-dependent increase with rising miRNA-21 levels. The assay demonstrated a biphasic linear response. A linear relationship was established within the range of 1 to 10 nM (Regression equation: $Y = 16\times + 53{,}118$, $R^2 = 0.965$, Fig. 4B) and a second linear range from 10 to 1000 pM (Regression equation: $Y = 20\times + 48{,}246$, $R^2 = 0.981$, Fig. 4C), where Y represents fluorescence intensity and X represents miRNA-21 concentration. The limit of detection (LOD) was calculated to be 2.88 pM, representing a more than 70-fold reduction compared to the group without the AMP probe (Fig. S4), based on the equation $LOD = 3\sigma/k$, where σ is the standard deviation of the fluorescence response from the negative control and k is the slope of the calibration curve in the lower concentration range.

To evaluate specificity, potential interferents (miRNA-141, miRNA-122, miRNA-155, M1 and M2) were tested. As shown in Fig. 4D, the fluorescence signals generated by these non-target miRNAs were considerably weaker than that of the target miRNA-21. Furthermore, the signal intensity of miRNA-21 spiked into samples containing these interferents at equivalent concentrations was comparable to that of miRNA-21 alone. These results confirm the high specificity of the sensing platform for miRNA-21, even in the presence of potential cross-reactive sequences.

Precision and accuracy were evaluated through spike-and-recovery experiments at low, medium and high miRNA-21 concentrations. The calculated recovery rates ranged from 95.5% to 108.6%, with relative standard deviations (RSDs) between 2.35% and 7.18% (detailed in Table S2). These data indicate that the method exhibits satisfactory accuracy and precision across the tested concentration range.

3.5. Analysis of real sample

To evaluate the practical applicability of the dumbbell-shaped probe-

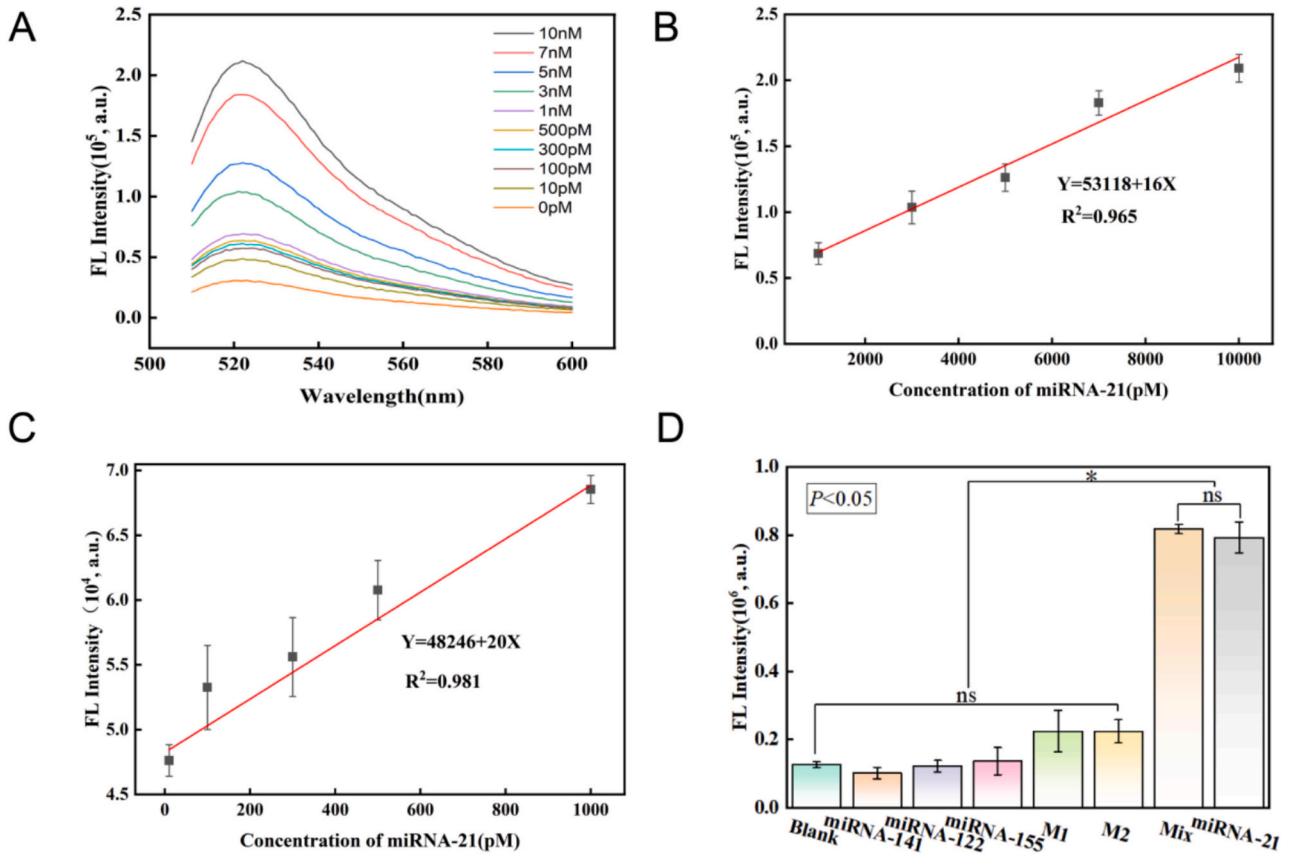


Fig. 4. Analytical performance of the miRNA-21 detection assay. FL intensity difference represents the signal relative to the background control. (A) Concentration-dependent fluorescence response to miRNA-21. (B) Calibration curve demonstrating linearity in the low-concentration range (1–10 nM; Regression: $Y = 16\times + 53{,}118$, $R^2 = 0.965$). (C) Calibration curve demonstrating linearity in the high-concentration range (10–1000 pM; Regression: $Y = 20\times + 48{,}246$, $R^2 = 0.981$). (D) Specificity assessment against non-target miRNAs (miRNA-141, miRNA-122, miRNA-155, M1 and M2) and mixtures (miRNA-21 + individual interferents) at equivalent concentrations. (Error bars represent standard deviation, SD; $n = 3$). ns indicates no significant difference. Analysis was performed using a two-independent-samples *t*-test. * indicates $P < 0.05$.

based biosensor, we performed miRNA-21 detection in clinically relevant samples. Human normal lung epithelial cells (BEAS-2B) expressing basal miRNA-21 levels, and human lung squamous carcinoma cells (H520) with intermediate miRNA-21 expression were selected as model systems (Fig. 5A). As demonstrated in Figs. 5B and C, the biosensor detected markedly elevated miRNA-21 expression in H520 cells compared to BEAS-2B controls ($P < 0.05$), confirming the capability of the proposed method to distinguish cancer cells from normal counterparts based on miRNA biomarker profiles. Finally, we compared the constructed method with the RT-qPCR gold standard and found that both exhibited the same trend of differences. (Fig. S5).

4. Discussion

In this study, we successfully developed a direct miRNA detection method through topological structure engineering and validated its technical feasibility. Compared with other analytical strategies, this study achieved relatively high sensitivity, lower detection complexity, and shorter detection time (Table S3). Future optimization efforts should focus on the following directions: first, further enhancing sensitivity, for example by integrating the AMP probe and the reporter probe into a single construct to improve signal amplification efficiency; second, validating the method in real clinical samples such as serum, plasma, or tissue lysates; third, expanding the multiplexing capability to enable simultaneous detection of multiple miRNAs rather than targeting only miRNA-21. Finally, increasing the number of experimental replicates would help reduce random errors, improve statistical power, and enhance the reproducibility of the results.

Although the above optimization strategies are intended to enhance the performance of the miRNA detection method, it is noteworthy that long non-coding RNAs (lncRNAs), besides miRNAs [27], also play a critical role in cancer initiation and progression [28]. Compared with miRNAs, the detection of lncRNAs faces greater technical challenges: these RNA molecules typically exceed 200 nucleotides in length, possess complex secondary and tertiary structures, and exhibit dynamic interactions with proteins—all of which significantly increase the difficulty of detection. Currently, clinical detection of lncRNAs relies primarily on reverse transcription quantitative PCR (RT-qPCR), a method that not only requires skilled operators but also depends on expensive thermocycling equipment, thereby greatly limiting its application in resource-limited settings. The development of CRISPR/Cas-based detection technologies offers a feasible alternative for lncRNA detection. More importantly, this technology is rapidly advancing toward wearable, portable, and real-time detection, opening up a new technological paradigm for point-of-care testing of nucleic acid biomarkers such as non-coding RNAs [29].

5. Conclusion

Here, through topological engineering of functional DNA probes, direct miRNA detection was achieved without additional steps such as reverse transcription and amplification. This one-pot CRISPR/Cas12a platform integrates toehold-mediated strand displacement, steric hindrance switching, and self-driven cascade signal amplification, demonstrating excellent analytical performance: a detection limit of 2.88 pM, high accuracy (recovery 95.5%–108.6%), good precision (RSD 2.35%–7.18%), and outstanding specificity. The method was successfully applied to quantify miRNA-21 levels in cultured cell lines, showing good agreement with the gold-standard RT-qPCR method. Overall, this study developed a direct microRNA detection method via topological engineering, confirming the technical feasibility of miRNA detection. The clinical applicability of this method requires extensive validation with clinical samples.

Ethical approval

Our study did not involve human participants, animals, or any ethical issues requiring approval.

Declaration of competing interest

The authors declare that they have no known competing financial

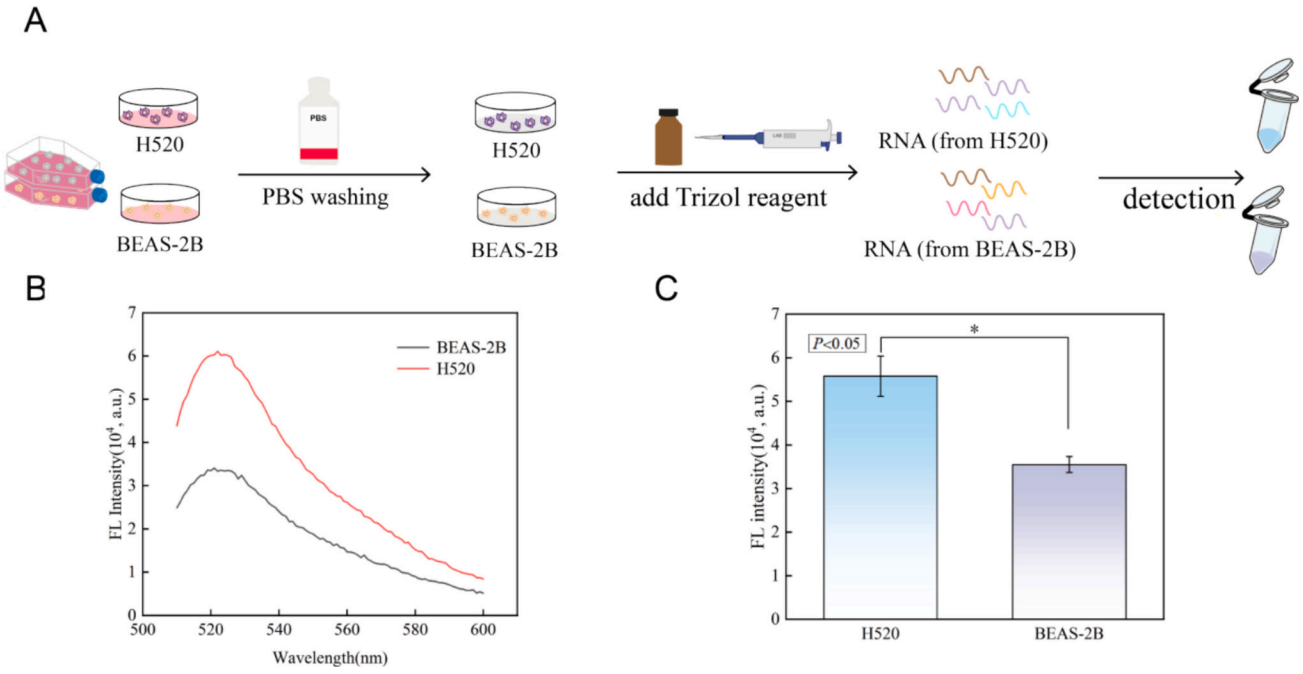


Fig. 5. Detection of miRNA-21 in cancer and normal cell lines. (A) Schematic workflow for miRNA extraction from cultured cells using Trizol reagent kit. (B) The fluorescence intensity detected by the constructed method for the two distinct cell lines.(C) Quantitative comparison of fluorescence signal showing markedly elevated miRNA-21 levels in lung squamous carcinoma cells (H520) versus normal lung epithelial cells (BEAS-2B). Error bars represent standard deviation (Error bars represent standard deviation, SD; $n = 3$). Analysis was performed using a two-independent-samples t-test. * indicates $P < 0.05$.

interests or personal relationships that could have appeared to influence the work reported in this paper.

Acknowledgments

This work was supported by Natural Science Foundation of Henan Province (Grant No. 242300421266) and Henan Provincial Selective Research Funding Program for Returned Scholars Studying Abroad (HNLX202605).

Appendix A. Supplementary data

Supplementary data to this article can be found online at https://doi.org/10.1016/j.saa.2026.128016.

Data availability

Data will be made available on request.

References

[1] M. Ratti, A. Lampis, M. Ghidini, et al., MicroRNAs (miRNAs) and long non-coding RNAs (lncRNAs) as new tools for cancer therapy: first steps from bench to bedside, Target. Oncol. 15 (3) (2020) 261–278, https://doi.org/10.1007/s11523-020-00717-x.
[2] L. Tomasello, R. Distefano, G. Nigita, et al., The MicroRNA family gets wider: the IsomiRs classification and role, Front. Cell Dev. Biol. (2021) 9, https://doi.org/10.3389/fcell.2021.668648.
[3] J.U.G. Wagner, L.S. Tombor, P.F. Malacarne, et al., Aging impairs the neurovascular interface in the heart, Science 381 (6660) (2023) 897–906, https://doi.org/10.1126/science.ade4961.
[4] B. Zhou, H. Yu, Y. Xue, et al., The spliceosome-associated protein CWC15 promotes miRNA biogenesis in *Arabidopsis*, Nat. Commun. 15 (1) (2024), https://doi.org/10.1038/s41467-024-46676-z.
[5] A.J. Gleichman, R. Kawaguchi, M.V. Sofroniew, et al., A toolbox of astrocyte-specific, serotype-independent adeno-associated viral vectors using microRNA targeting sequences, Nat. Commun. 14 (1) (2023), https://doi.org/10.1038/s41467-023-42746-w.
[6] J.T.-S. Chow, A. Desjardins, D.K.C. Lee, et al., A microRNA CRISPR screen reveals microRNA-483-3p as an apoptotic regulator in prostate cancer cells, Cell Death Dis. 16 (1) (2025), https://doi.org/10.1038/s41419-025-08098-7.
[7] L. Drago, L.R. De La Motte, L. Deflorio, et al., Systematic review of bidirectional interaction between gut microbiome, miRNAs, and human pathologies, Front. Microbiol. (2025) 16, https://doi.org/10.3389/fmicb.2025.1540943.
[8] S. Shin, Y. Jung, H. Uhm, et al., Quantification of purified endogenous miRNAs with high sensitivity and specificity, Nat. Commun. 11 (1) (2020), https://doi.org/10.1038/s41467-020-19865-9.
[9] Y. Gao, S. Zhang, C. Wu, et al., Self-protected DNAzyme walker with a circular bulging DNA shield for amplified imaging of miRNAs in living cells and mice, ACS Nano 15 (12) (2021) 19211–19224, https://doi.org/10.1021/acsnano.1c04260.
[10] K.A. Preethi, S.C. Selvakumar, K. Ross, et al., Liquid biopsy: exosomal microRNAs as novel diagnostic and prognostic biomarkers in cancer, Mol. Cancer 21 (1) (2022), https://doi.org/10.1186/s12943-022-01525-9.
[11] H.S. Chawra, M. Agarwal, A. Mishra, et al., MicroRNA-21's role in PTEN suppression and PI3K/AKT activation: implications for cancer biology, Pathol. Res. Pract. 254 (2024), https://doi.org/10.1016/j.prp.2024.155091.
[12] L. Hu, J. Wang, Z. Hao, et al., MicroRNA-21 promotes the viability, proliferation and milk fat synthesis of ovine mammary epithelial cells by targeting PDCD4, Int. J. Mol. Sci. 26 (4) (2025), https://doi.org/10.3390/ijms26041460.
[13] P. He, W. Han, C. Bi, et al., Many birds, one stone: a smart nanodevice for ratiometric dual-spectrum assay of intracellular microRNA and multimodal synergetic cancer therapy, ACS Nano 15 (4) (2021) 6961–6976, https://doi.org/10.1021/acsnano.0c10844.
[14] S.-P. Hwang, K. Barondeau, C. Denicourt, Protocol to detect m22G modification on single tRNA iso-decoders by immuno-northern blotting, STAR Protoc. 6 (3) (2025), https://doi.org/10.1016/j.xpro.2025.103924.
[15] C. Yao, Q. Wang, X. Lu, et al., Hydrogel-based microdroplet ensembles encapsulating multiplexed EXPAR assays for trichromic digital profiling of microRNAs and in-depth classification of primary urethral cancers, Nano Lett. 24 (49) (2024) 15861–15869, https://doi.org/10.1021/acs.nanolett.4c04898.
[16] M. Li, F. Yin, L. Song, et al., Nucleic acid tests for clinical translation, Chem. Rev. 121 (17) (2021) 10469–10558, https://doi.org/10.1021/acs.chemrev.1c00241.
[17] F. Yang, Q. Yang, L. Yang, et al., Endogenous microRNA accurate diagnostics to guide photothermal therapy, Anal. Chem. 94 (17) (2022) 6599–6606, https://doi.org/10.1021/acs.analchem.2c00712.
[18] A. Ganguli, A. Mostafa, J. Berger, et al., Rapid isothermal amplification and portable detection system for SARS-CoV-2, Proc. Natl. Acad. Sci. USA 117 (37) (2020) 22727–22735, https://doi.org/10.1073/pnas.2014739117.
[19] O.O. Abudayyeh, J.S. Gootenberg, CRISPR diagnostics, Science 372 (6545) (2021) 914–915, https://doi.org/10.1126/science.abi9335.
[20] B. Paul, G. Montoya, CRISPR-Cas12a: functional overview and applications, Biom. J. 43 (1) (2020) 8–17, https://doi.org/10.1016/j.bj.2019.10.005.
[21] L. Yin, S. Man, S. Ye, et al., CRISPR-Cas based virus detection: recent advances and perspectives, Biosens. Bioelectron. (2021) 193, https://doi.org/10.1016/j.bios.2021.113541.
[22] Z. Huang, C.J. Lyon, J. Wang, et al., CRISPR assays for disease diagnosis: progress to and barriers remaining for clinical applications, Adv. Sci. 10 (20) (2023), https://doi.org/10.1002/advs.202301697.
[23] J. Shen, X. Zhou, Y. Shan, et al., Sensitive detection of a bacterial pathogen using allosteric probe-initiated catalysis and CRISPR-Cas13a amplification reaction, Nat. Commun. 11 (1) (2020), https://doi.org/10.1038/s41467-019-14135-9.
[24] J. Zeng, P. Liu, J. Du, et al., Split crRNA-motivated amplification-free RNA testing with CRISPR–Cas12a, Sci. China Chem. 68 (2) (2024) 789–801, https://doi.org/10.1007/s11426-024-2241-1.
[25] Y. Chen, X. Wang, J. Zhang, et al., Split crRNA with CRISPR-Cas12a enabling highly sensitive and multiplexed detection of RNA and DNA, Nat. Commun. 15 (1) (2024), https://doi.org/10.1038/s41467-024-52691-x.
[26] J. Wang, X. Ye, Y. Liu, et al., Regulating cleavage activity and enabling microRNA detection with split sgRNA in Cas12b, Nat. Commun. 16 (1) (2025), https://doi.org/10.1038/s41467-025-61748-4.
[27] P. Thomas, S.C. Selvakumar, K.A. Preethi, et al., Expression profiling of signal transducer and activator of transcription3 in oral squamous cell carcinoma in South Indian population, Minerva Dent. Oral Sci. 73 (1) (2024) 37–44, https://doi.org/10.23736/s2724-6329.23.04840-4.
[28] K.P. A, P.P.A.S. Usman, D. Sekar, OIP5-AS1 expression profiles in different stages of oral squamous cell carcinoma, Arch. Oral Biol. (2025) 180, https://doi.org/10.1016/j.archoralbio.2025.106403.
[29] K.P. Ameya, K. Ross, D. Sekar, Wearable nanopatch platforms for real-time miRNA sensing and editing: a vision for next-generation cancer management, Med. Oncol. 42 (12) (2025), https://doi.org/10.1007/s12032-025-03091-8.